Phase Constitution Characteristics of the Fe-Al Alloy Layer in the HAZ of Calorized Steel Pipe

Controlling the aluminum content of the surface layer of calorized steel pipe substantially improves weldability

L. YAJIANG, Z. ZENGDA AND W. XING

ABSTRACT. Mechanical properties of the welding region and phase constitution characteristics in the iron-aluminum (Fe-Al) alloy layer of calorized steel pipes were researched by means of metallography, which included the use of scanning electron microscopy (SEM), transmission electron microscopy (TEM), electron probe microanalysis (EPMA) and an X-ray diffractometer. Experimental results indicated that the Fe-Al alloy layer of calorized steel pipe was mainly composed of an FeAl phase, an Fe_3Al phase and an α-Fe(Al) solid solution, and the microhardness in the Fe-Al coating was 600–310 HM from the surface layer to the inside. There were no higher aluminum content phases, such as brittle $FeAl_2$, Fe_2Al_5 and $FeAl_3$. By controlling the aluminizing process parameters, the ability to bear deformation and weldability of the calorized steel pipe were remarkably improved.

Introduction

Aluminum-coated steels exhibit excellent resistance to oxidation and corrosion in some media, and may remarkably increase the service life of petrochemical equipment. In recent years, numerous investigators have paid close attention to the properties of the aluminum-coated steels (Refs. 1–3). The welding performance and phase constitution of the aluminum-coated steels differ greatly for the different aluminizing processes. The Fe-Al state diagram shows that three intermetallic compounds (namely $FeAl_2$, Fe_2Al_5 and $FeAl_3$) would be stable at the aluminizing temperature of 600–800°C (in a pure Al bath). But, a thick Fe-Al alloy layer grown under normal operating conditions in pure and iron-containing aluminum melts cannot withstand bending and welding operations.

There are two main methods for welding aluminum-coated steels: 1) removing, by a mechanical method, the Fe-Al alloy layer in the region of the joint before welding , then welding using an ordinary electrode, and spraying a layer of aluminum in the welded zone after welding; and 2) welding with a stainless steel electrode or a special electrode of an aluminum-coated steel. This paper presents a study of welding the latest types of aluminum-coated steel pipes. The objective of this investigation is to stabilize the Fe-Al alloy layer by examining the possibility of eliminating or minimizing the pure Al content on the surface of workpiece. It is shown that by controlling a series of aluminizing process parameters, the aluminum content and phase constitution of the Fe-Al alloy layer may be effectively controlled, with the elimination of the brittle $FeAl_2$, Fe_2Al_5 and $FeAl_3$ phases in the Fe-Al alloy layer. As a result, the deformation resistance of the aluminum-coated steel may be greatly enhanced and, especially, the weldability may be remarkably improved. Investigations on the nature and type of the Fe-Al intermetallics formed were carried out, not only on the surface of the coating, but also on layers at different depths through removal of the layers followed by X-ray diffraction and optical examination.

LI Yajiang is Associate Professor, ZOU ZENGDA is Professor and WEI XING is Engineer, Materials Engineering Department, Shandong University of Technology, Jinan, People's Republic of China.

KEY WORDS

Calorized Steel
Welding
Heat-Affected Zone
Microstructure
Fe-Al Alloy Layer
Phase Constitution

Experimental Method

Base metals used in the test were low-carbon aluminum-coated steel pipe (114-mm diameter, 6-mm wall thickness) and Cr-Mo aluminum-coated steel pipe (114-mm diameter, 10-mm wall thickness), used in the petrochemical industry. The chemical composition of the base metals is shown in Table 1. The aluminizing process involved successive stages of workpiece surface pretreatment, preparation of the primary aluminizing compound, thermal diffusion treatment (by means of electric-induction heating) and surface cleaning of the workpiece. The calorizing parameters were 1050°C (heating temperature) and 15 min (holding time at the temperature), followed by slow cooling. The conventional hot dip aluminizing process needs about 4 h. The welding parameters, using a Cr23-Ni13-type electrode in the experiments, are shown in Table 2.

Samples of the aluminum-coated steel pipe and the weld joint zone were cut mechanically. The mechanical properties of the aluminum-coated steel pipes and the weld joints were measured by tensile and bend testing. Microstructures and microhardness of the Fe-Al alloy layer in the heat-affected zone (HAZ) were analyzed using optical microscopy and a microsclerometer. Aluminum concentration distribution and phase constitution in the coating were further analyzed by scanning electron microscopy, electron probe microanalysis, transmission electron microscopy and X-ray diffraction.

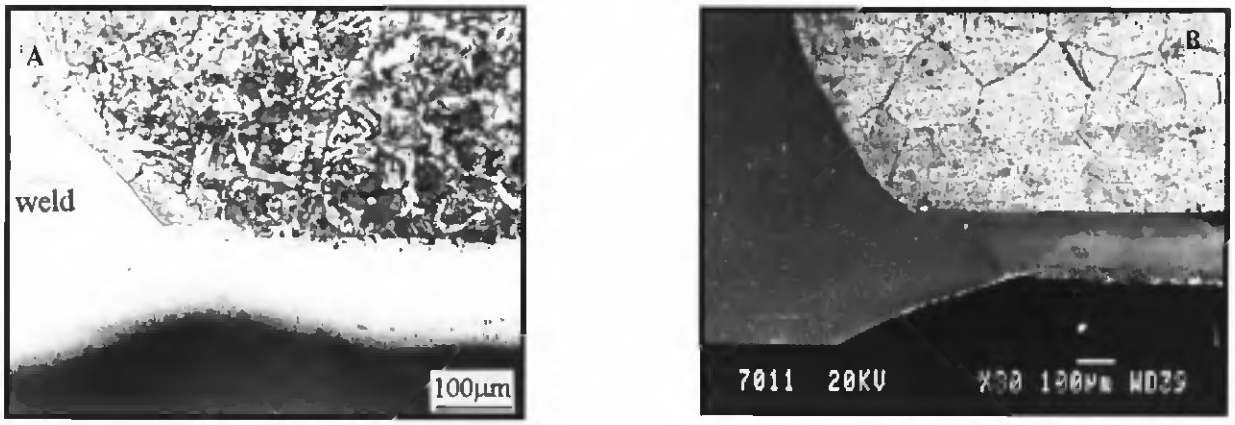

Fig. 1 — Microstructures in the welded zone of calorized steel pipe. A — Microstructure; B — SEM.

Experimental Results and Discussion

Mechanical Properties

An experiment to determine the mechanical properties of the two kinds of aluminum-coated steel pipes and their welded joints was made on a 20-tonne tensile testing machine. The test results are shown in Table 3. Clearly, mechanical properties of both kinds of steel pipes are not reduced after the aluminizing process. Before and after aluminizing, the mechanical properties of such steel pipes do not differ greatly. The mechanical properties of the weld metals can be assured.

Cold-bend tests were made by the three-point bend method to determine the deformation resistance of the Fe-Al alloy layer on aluminum-coated steel pipes. The original Fe-Al alloy layer on both the inside and outside walls of the calorized steel specimens remained in good condition. Cold-bend angles were 10 and 90 deg, respectively. After the cold-bend deformation tests, specimens were etched in a 30% nitric acid and water solution and then examined with low magnification (5–10X). Both types of calorized steel pipes may be bent to 30 deg without any tiny cracks appearing in the Fe-Al alloy layer. The Fe-Al coating of the common aluminum-coated steel pipe (e.g., hot dip aluminized steel) produced cracks very easily as a result of the existing brittle phases. The bend specimen of the hot dip aluminum-coated steel pipe may only be bent to about 10 deg. Furthermore, a distorted specimen that had been subjected to an average stress of 500 MPa and an elongation of 8% was cut from the calorized steel pipe. It was subsequently etched in a 30% nitric acid-water solution, and the Fe-Al alloy layer was again examined with a 5–10X magnifying glass. No tiny cracks were found. The results of the cold-bend deformation tests indicated that the Fe-Al alloy layer on the calorized steel pipes possessed a reasonable degree of deformation resistance and good ductility, both favorable to weldability.

Microstructural Characteristics

Microstructures of the welded joint zone of low-carbon calorized steel pipe are shown in Fig. 1A and B. The Fe-Al alloy layer continuously transited from the heat-affected zone to the weld metal.

The thickness of the Fe-Al alloy layer on the inside and outside walls of low-carbon calorized steel pipe was 0.15–0.22 mm and 0.14–0.20 mm, respectively. The thickness of the Fe-Al alloy layer on the inside and outside walls of Cr-Mo calorized steel pipe was 0.12–0.16 mm and 0.10–0.14 mm, respectively. The base metal microstructure of the low-carbon aluminum-coated steel pipe exhibited both ferrite and pearlite, there being no other harmful

Table 1 — The Chemical Composition of the Base Metals Used in the Experiment

	C	Mn	Si	Cr	Mo	S	P
Low-carbon steel	0.18	0.45	0.28	—	—	0.018	0.022
Cr-Mo steel	0.14	0.48	0.36	5.00	0.55	0.016	0.020

Table 2 — Welding Parameters Used in the Experiment

Calorized steel	Electrode	Welding voltage (V)	Welding current (A)	Polarity
Low-carbon calorized steel pipe	E1-23-13-16 (Φ3.2 mm)	26–28	85–100	AC
Cr-Mo calorized steel pipe	E1-23-13-16 (Φ3.2 mm)	26–30	85–110	AC

Table 3 — Mechanical Properties of the Aluminum-Coated Steel Pipes

	Specimen state	Tensile strength (MPa)	Elongation (%)	Cold bend angle (°C) Positive bend	Back bend
Low-carbon calorized steel pipe	Before aluminizing	392–436	20.0–21.5	—	—
	After aluminizing	421–445	19.5–22.5	—	—
	Welded joint	435–465 (447)[a]	24.7–27.5 (26)	60	60
Cr-Mo calorized steel pipe	Before aluminizing	540	17.5	—	—
	After aluminizing	525–560	19.5–22.0	—	—
	Welded joint	510–562 (541)	19.5–22.5 (20.2)	30	30

(a) Figures in parentheses are the experimental average value.

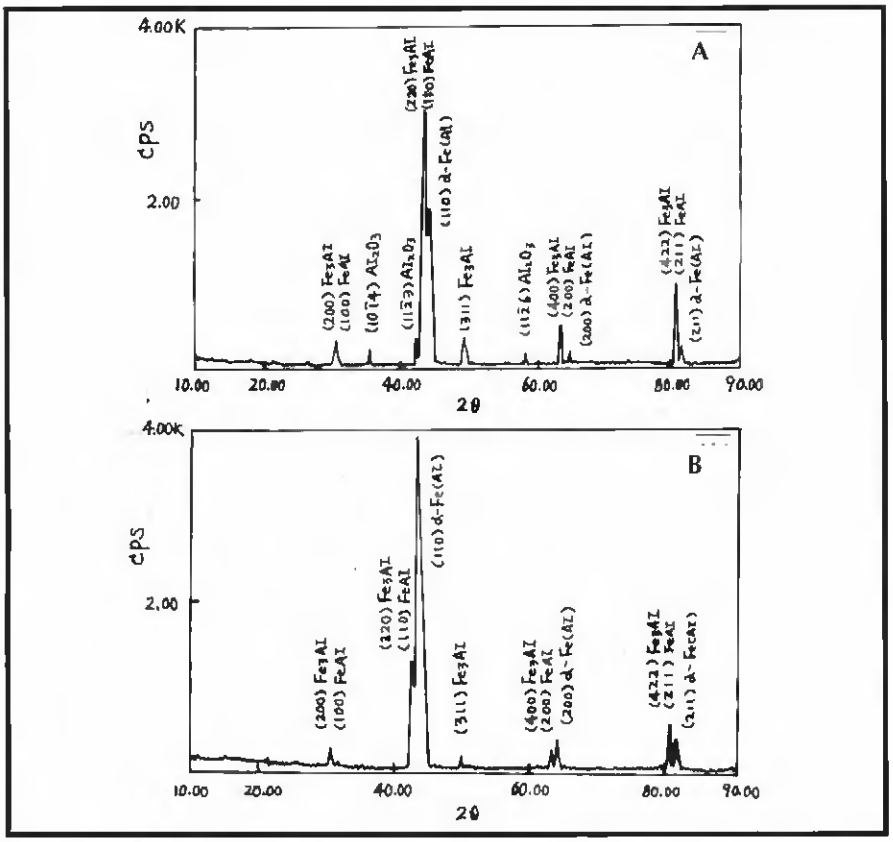

Fig. 2 — X-ray diffraction diagram in the Fe-Al alloy layer (diffraction condition: copper target, 40 KV, 150 mA). A — Surface layer; B — depth from the surface layer was 50 µm.

Table 4 — Microhardness, Al and Fe Content in the Fe-Al Alloy Layer

Measuring point	Distance from surface layer (µm)	Region	Microhardness (HM)	Al (wt-%)	Fe (wt-%)
1	0	Coating, outer edge	—	28.0	72.0
2	8	Coating, outer edge	—	26.5	73.1
3	15	Coating, outer edge	600	—	—
4	30	Coating, middle part	490	23.2	76.4
5	45	Coating, middle part	475	—	—
6	52	Coating, middle part	471	21.6	77.8
7	75	Coating, middle part	415	—	—
8	98	Coating, middle part	398	16.7	82.6
9	125	Coating	393	9.8	89.5
10	144	Coating	364	6.8	92.6
11	180	Coating, boundary with base	350	—	—
12	190	Coating, boundary with base	320	1.3	97.5

Table 5 — Aluminum Content and Microhardness of Intermetallic Compounds in the Fe-Al System

Phase	Al (wt-%) According to state diagram	Al (wt-%) Chemical analysis	Microhardness (HM)
Fe_3Al	13.87	14.04	350
FeAl	32.57	33.64	640
$FeAl_2$	49.13	49.32	1030
Fe_2Al_5	54.71	54.92	820
$FeAl_3$	59.18	59.40	990
Fe_2Al_7	62.93	63.32	1080

phase present that could affect weldability. The base metal microstructure of the Cr-Mo aluminum-coated steel pipe consisted of bainite and martensite after normalizing. Annealing was employed to further improve the weldability of the Cr-Mo aluminum-coated steel pipe. After annealing, the basic microstructure was pearlite. Annealing of the Cr-Mo aluminum-coated steel pipe greatly improved both the microstructure and other properties, especially that of weldability, while properties of the Fe-Al alloy layer remained unchanged.

The microhardness of the Fe-Al alloy layer was measured using a microsclerometer using a 50-g load and a load time of 12 s. The microhardness was reduced gradually from the outer surface layer to the base metal (Table 4). When the depth of the Fe-Al alloy layer was less than 60 µm, the microhardness varied in general between 470 and 600 HM. The microhardness near the coating boundary with the base metal was 320–350 HM. The base metal microhardness was 140 HM for ferrite and 220 HM for pearlite. As a result of this lower microhardness in the Fe-Al alloy layer, the aluminum-coated steel pipes exhibited a good ability to bear ductile deformation.

The oxidation resistance of the Fe-Al alloy layer is determined by the aluminum content. To form a compact and continuous alumina film, 8–25 wt-% aluminum is required to be present at a temperature in excess of 1000°C; 5–8 wt-% aluminum is required at 800°C (Ref. 4). The composition of the Fe-Al alloy layer was analyzed from the surface of the coating to the interior at successive depths by means of SEM and EPMA. The distance between each point of measurement was 46 µm, using wavelength dispersive rather than energy dispersive spectroscopy. The experimental results are presented in Table 4. The aluminum content in the Fe-Al alloy layer reduces with increasing depth from the coating. The aluminum content of the surface layer is about 28 wt-%. When the depth from the surface layer has reached no more than 140 µm, the aluminum content is in excess of 8 wt-%. The effective thickness of the Fe-Al alloy layer can satisfy the necessary requirements for both heat and corrosion resistance.

By analyzing the microhardness and the aluminum content of the Fe-Al alloy layer at different depths, Fe-Al intermetallic compounds that could exist in the coating may be ascertained. The aluminum content and microhardness of different intermetallic compounds in the Fe-Al system are presented in Table 5 (Refs. 5, 6).

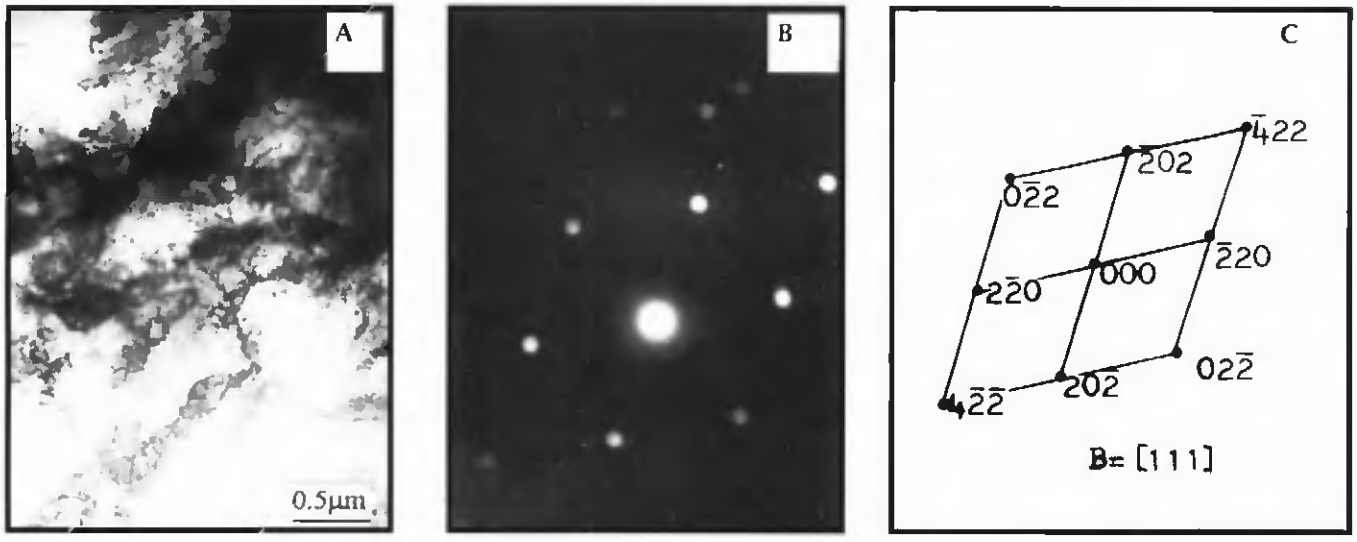

Fig. 3 — Structure characteristics of Fe_3Al in the Fe-Al alloy layer. A — TEM morphology (25,000X); B — electron diffraction pattern; C — index schematic diagram.

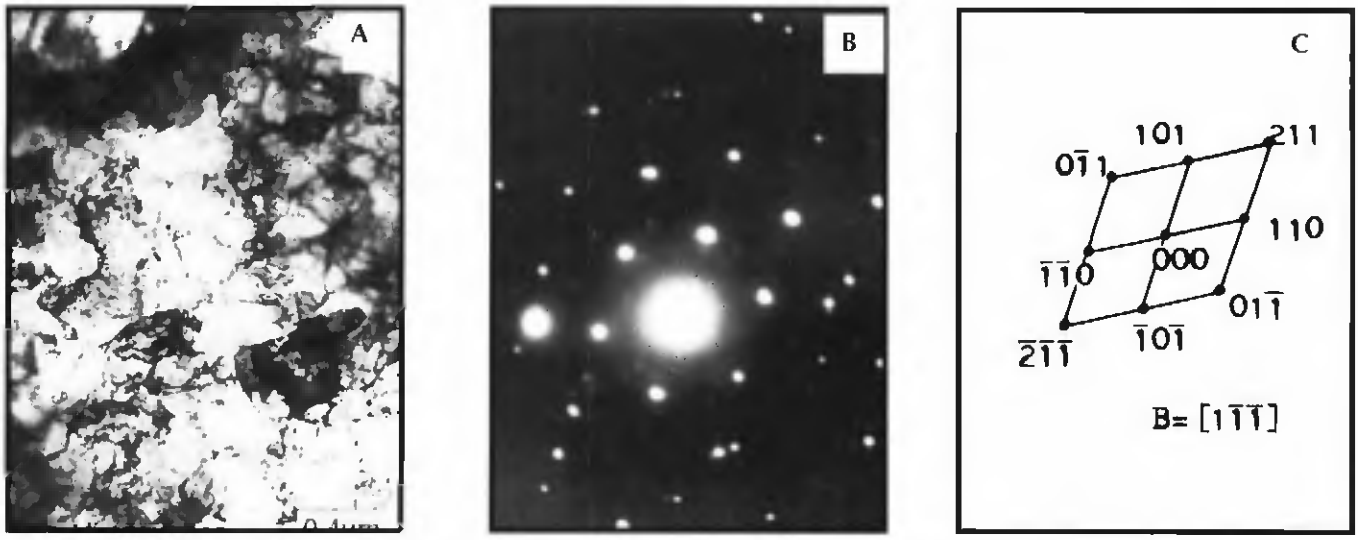

Fig. 4 — Structure characteristics of FeAl in the Fe-Al alloy layer. A — TEM morphology (25,000X); B — electron diffraction pattern; C — index schematic diagram.

Phase Constitution in the Fe-Al Alloy Layer

The Fe-Al alloy layer was further analyzed in discreet layers with the aid of an X-ray diffractometer, using a copper target (Cu-Ka). The working voltage was 40 kV and the working current was 150 mA. Radiation employed was monochromated rather than filtered. The experimental results are presented in Fig. 2A and B. The crystal-plane spacings (d values) corresponding to the diffraction peaks in the diagrams have been computed. These computed results have been compared with the crystal-plane spacings (d values) of FeAl phase, Fe_3Al phase, α-Fe(Al) solid solution and Al_2O_3, which have been published by the Joint Committee on Powder Diffraction Standards (JCPDS) (Ref. 7). The results indicate that the measured values are close to the d spacing values published by JCPDS (Table 6).

FeAl (bcc) and Fe_3Al (fcc) phases are dominantly present in the Fe-Al alloy layer observed in this research; other phases, such as $FeAl_2$, Fe_2Al_5 and $FeAl_3$, are not expected to exist in the alloy layer. Usually, the aluminum-rich compounds form at the outer surface and compounds progressively richer in iron should form subsequently (Ref. 5). However, in many layers, a mixture of compounds form, some richer in aluminum and some in iron. Further holding of the aluminized sample at 950°C for 30 min and water quenching made no significant difference to the phase constitution in the Fe-Al alloy layer.

Fe_3Al and FeAl in the Fe-Al alloy layer are stable over a range of compositions. At equilibrium, Fe_3Al occurs as a DO_3 structure between 13.9 and 20 wt-% Al at room temperature, while FeAl has the B2 structure and exists between 20 and 36 wt-% Al. Although the ductility of the DO_3 structure is greater than that of the B2 structure, it is only stable up to 540°C. Above 540°C, the B2 structure is stable (Ref. 8). To clarify further the morphology of the component phases and combined state of the boundary plane in the Fe-Al alloy layer, microstructures of film samples from the Fe-Al alloy layer were ana-

Table 6 — Experimental Results of X-ray Diffraction for the Fe-Al Alloy Layer

Measured values	Data from JCPDS											
	FeAl			Fe_3Al			α-FeAl			Al_2O_3		
d (nm)	d (nm)	hkl	I/I_o	d (nm)	hkl	I/I_o	d (nm)	hkl	I/I_o	d (nm)	hkll	I/I_o
—	—	—	—	0.334	111	60	—	—	—	—	—	—
0.291	0.289	100	12	0.289	200	50	—	—	—	—	—	—
0.256	—	—	—	—	—	—	—	—	—	0.255	1014	90
0.210	—	—	—	—	—	—	—	—	—	0.209	1123	100
0.206	0.204	110	100	0.204	220	100	—	—	—	—	—	—
0.203	—	—	—	—	—	—	0.203	110	100	—	—	—
0.180	—	—	—	0.179	311	20	—	—	—	—	—	—
—	—	—	—	—	—	—	—	—	—	0.174	0224	45
—	0.167	111	4	0.167	222	10	—	—	—	—	—	—
0.159	—	—	—	—	—	—	—	—	—	0.160	1126	80
0.146	0.145	200	8	0.145	400	80	—	—	—	—	—	—
0.143	—	—	—	—	—	—	0.143	200	20	—	—	—
—	—	—	—	—	—	—	—	—	—	0.140	1234	30
—	—	—	—	—	—	—	—	—	—	0.137	0330	50
0.118	0.118	211	20	0.118	422	90	—	—	—	—	—	—
0.116	—	—	—	—	—	—	0.117	211	30	—	—	—

lyzed by TEM and electron diffraction. TEM morphology, the electron diffraction pattern and schematic index diagrams of the component phases in the Fe-Al alloy layer, taken from the [111] and [1$\bar{1}\bar{1}$] directions, are shown in Figs. 3 and 4, respectively. The black region in the TEM photograph was Fe_3Al and FeAl phases, the white region in the photograph was an α-Fe(Al) solid solution that possesses bcc structure (the lattice constant is 0.287 nm).

Microstructural morphology of FeAl, Fe_3Al and α-Fe(Al) solid solution near the surface of the Fe-Al alloy layer was analyzed by high-resolution multiple SEM and TEM. The test results indicate that the component phases were composed of inlaid subcrystal grains — Figs. 3A and 4A. There was a dislocation twin boundary, rather than a boundary involving interfacial dislocations, at the position of the component phase boundary. No microscopic defects, such as pores and cracks, were found in the FeAl phase, Fe_3Al phase and α-Fe(Al) solid solution. This indicated that the phase constitution of the Fe-Al alloy layer was compact. This is favorable for oxidation resistance and corrosion resistance of the Fe-Al alloy layer of aluminum-coated steel.

Phase construction analysis indicated that the Fe-Al alloy layer of calorized steel pipe was mainly composed of α-Fe(Al) solid solution, Fe_3Al phase, FeAl phase and a small amount of Al_2O_3 (Table 7). The Fe_3Al and FeAl phases possess characteristics of fine crystal grains, based on features of the polycrystal diffraction pattern.

Further analysis indicated that the FeAl phase was not the main component of the Fe-Al coating. Brittle phases that contained more aluminum, such as $FeAl_2$ (49.13 wt-% Al), Fe_2Al_5 (54.71 wt-% Al) and FeAl3 (59.18 wt-% Al), did not exist in the Fe-Al alloy layer. Weld cracks and deterioration of weld performance formerly caused by these brittle phases in hot dip, aluminum-coated steel pipes were effectively eliminated. As a result, the ability to bear ductile deformation and the weldability of aluminum-coated steel pipes were remarkably improved.

Table 7 — Phase Composition of Different Diffraction Layer Faces in the Fe-Al Alloy Layer

Depth from the surface layer (μm)	Phase composition
0	Al_2O_3, FeAl, Fe_3Al and α-Fe(Al) solid solution
50	FeAl, Fe_3Al and α-Fe(Al) solid solution
120	FeAl, Fe_3Al and α-Fe(Al) solid solution
180	Fe_3Al and α-Fe(Al) solid solution

Conclusions

1) The average thickness of the Fe-Al alloy layer on the calorized steel pipes was 0.14–0.22 mm. The aluminum content of the outermost layer was about 28 wt-%. The aluminum content in the Fe-Al alloy layer is also reduced with depth from the surface layer. Microhardness in the Fe-Al alloy layer ranged from 600–320 HM taken from the surface to the inner side.

2) The strength properties of the calorized steel pipes did not vary greatly before and after aluminizing. The necessary mechanical properties of the weld metal can be easily assured. The Fe-Al alloy layer continuously transited from the HAZ to the weld metal and possessed a reasonable ability to resist oxidation and corrosion.

3) The Fe-Al alloy layer of the calorized steel pipe was mainly composed of compact FeAl phase, Fe_3Al phase and α-Fe(Al) solid solution, according to the depth from the surface layer of the coating. There were no brittle $FeAl_2$, Fe_2Al_5 or $FeAl_3$ phases containing more aluminum in the Fe-Al alloy layer. This is favorable to weldability and the ability to bear deformation in equipment installation.

References

1. Okamoto, H., and Paul, A. B. 1971. Phase relationship in the iron-rich Fe-Al alloys. *Metallurgical Transactions* 2(2): 569–574
2. Linnert, G. E. 1964. Techniques for welding aluminum-coated steel. *Welding Design and Fabrication* 37(9): 50–54
3. Tjong, S. C. 1986. Some aspects of the aluminide coating on Fe-18Cr alloy. *Werkstoffe und Korrosion* 37(10): 591–595.
4. Saegusa, F., and Lee, L.1966. Oxidation of iron-aluminium alloys in the range 500–1000°C. *Corrosion* 22 (6): 168-177.
5. Bahadur, A., and Mohanty, O. N. 1990. Structural study of calorized coatings on mild steel. *Materials Transactions*, JIM 31(11): 948–953.
6. Kangsheng, H., and Xiongfu, C. 1986. *Welding of Dissimilar Metals*. Beijing, Mechanical Industry Press.
7. Xiong, F. 1981. *X-ray Metallography*. Tianjin Univ. Press.
8. Fair, G. H., and Wood, J. V. 1994. Mechanical alloying of Fe-Al intermetallics in the DO_3 composition range. *Journal of Materials Science* 29: 1935–1939.